

A Comparison of the Fermionic Overlap-Dirac Operator and Pure Gauge Field Definitions of the Quenched Topological Susceptibility in the Schwinger Model

Lera Sapozhnikova^{a,c} James Beacham^{b,c}

^a*Faculty of Physics, M.V. Lomonosov Moscow State University,
Moscow, Russia*

^b*Department of Physics, University of California, Santa Cruz, CA, USA*

^c*John von Neumann Institute for Computing, NIC, DESY, Zeuthen, Germany*

September 17, 2007

Abstract

An investigation of the topological susceptibility, which can be related to the mass of the η' meson, is presented. We use two different definitions of the topological charge and compare the topological susceptibility with the theoretically predicted value in the continuum limit. We find that our results correspond reasonably well with the predicted value.

1 Introduction

The η' meson is a particle of considerable research interest within the high energy physics community. Calculation and conjecture regarding the generation of its mass is an area of active inquiry, and, since the generation of the η' mass is of a non-perturbative nature, much of this research is done within the framework of lattice QCD and involves large-scale numerical simulations. Our goal was to analyze gauge field configurations and, in particular, to take measurements regarding a quantity known as the topological susceptibility χ_{topo} .

This report is organized as follows: **Section 1** discusses the requisite theory. **Section 2** presents our results, including values for χ_{topo} in the continuum limit. **Section 3** offers our conclusions and suggests future work.

2 Theory

2.1 From Quantum Mechanics to Quantum Field Theory to QCD to the Schwinger Model

In canonical quantum mechanics, the fundamental objects are wave functions ψ that are solutions to the Schrödinger equation. Schrödinger's original formulation involved the Hamiltonian H of the system:

$$H|\psi(t)\rangle = i\hbar \frac{\partial}{\partial t} |\psi(t)\rangle,$$

Solutions, then, are of the form $|\psi(t)\rangle = e^{-iHt/\hbar} |\psi(0)\rangle$.

An equivalent formulation of quantum mechanics, though, is the path integral version of Richard Feynman, in which the essential objects are *paths* between a beginning position x_a and an ending position x_b , each of which contributes appropriately to the total probability amplitude of a particle traveling between x_a and x_b . The quantum theory is expressed in terms of an action integral which is, in turn, determined from the Lagrangian of the system in question. In particular, the appropriate weight of a path is given by its corresponding action through $e^{-iS[a,b]/\hbar}$.

A most fundamental object in Feynman's formulation of quantum mechanics is the *kernel*, which describes the path taken by a particle in going from x_a to x_b . In the formulation of Feynman and Hibbs [1], the essential ingredient is that *all* possible paths from x_a to x_b have to be considered. Each of these paths is appropriately weighted by $e^{-iS[a,b]/\hbar}$. The fundamental objects, then, are no longer wave functions that live in Hilbert space, but *probability amplitudes* expressed in terms of path integrals over a *set of functions*, which are the particle's paths.

For instance, the Lagrangian for the one dimensional harmonic oscillator is

$$\mathcal{L} = \frac{m}{2}(\dot{x}^2 - \omega^2 x^2)$$

and the corresponding action is

$$S = \int \mathcal{L}(x, \dot{x}) dt. \tag{1}$$

If we wish to calculate the kernel of this system of a particle traveling from x_a at time t_a to x_b at time t_b , we note (as Feynman originally did) that the integral over all the paths of the particle does not require explicit knowledge of the classical path taken. That is, the kernel is written

$$K(b, a) = \int_a^b \exp \left[\frac{i}{\hbar} \int_{t_a}^{t_b} \mathcal{L}(\dot{x}, x, t) dt \right] \mathcal{D}x(t), \tag{2}$$

where $\mathcal{D}x(t)$ indicates that the integral is over all possible paths of the particle.

The classical contribution can be factored out of (2) and the kernel is thus determined up to some function of t_b and t_a ,

$$K(b, a) = e^{\frac{i}{\hbar} S_{cl}[b, a]} F(t_b, t_a),$$

where $S_{cl}[b, a]$ is the classical action. It can be shown, although non-trivially (please ask to see our many pages of hand-calculation), that the kernel for the harmonic oscillator is

$$K_{HO}(b, a) = \left(\frac{m\omega}{2\pi i\hbar \sin \omega T} \right)^{\frac{1}{2}} \exp \left[\frac{im\omega}{2\hbar \sin \omega T} \left[(x_a^2 + x_b^2) \cos \omega T - 2x_a x_b \right] \right] \quad (3)$$

where $T = t_b - t_a$. Of course, in the standard formulation of quantum mechanics, the one dimensional harmonic oscillator can be solved in a much more straightforward manner via a linear combination of wave functions that are the direct solutions of the Schrödinger equation. In this case, the path integral approach is perhaps a bit unwieldy and undesirable.

In a field theoretical approach, though, path integrals play an essential role. A quantum field theory is most properly treated by considering a Lagrangian rather than Hamiltonian formalism, since Lagrangian dynamics more adequately respects the natural symmetries (which relate to conserved quantities) inherent in many field theories. Since path integrals utilize this same Lagrangian formalism, they are a natural choice for formulating the theory of and performing calculations on a quantized field.

As mentioned, Feynman's kernel K corresponds to a probability amplitude U of a particle traveling from x_a at time t_a to x_b at time t_b . Recall that, using traditional Hamiltonian formalism, this can be expressed (now using bra-ket notation) as

$$U(x_b, x_a; T) = \langle x_b | e^{-iHT/\hbar} | x_a \rangle. \quad (4)$$

We are interested in the *total* amplitude of moving from x_a to x_b , which, as noted above, amounts in Feynman's path integral approach to a consideration of *every possible path*. Following Peskin and Schroeder [2], for example, we can write U as

$$U(x_b, x_a; T) = \sum_{\text{all paths}} e^{i \cdot (\text{phase})} = \int \mathcal{D}x(t) e^{i \cdot (\text{phase})}. \quad (5)$$

If we now incorporate Feynman's concept of the path integral, this complex phase can be interpreted as the action, $S[x(t)]$. We thus have

$$\langle x_b | e^{-iHT/\hbar} | x_a \rangle = U(x_b, x_a; T) = \int \mathcal{D}x(t) e^{iS[x(t)]/\hbar}. \quad (6)$$

It can be shown ([2], pp 277 - 279), that these two definitions satisfy the same differential equation with the same initial condition and are therefore equivalent.

To move to a quantum *field* theory, then, we re-write U in terms of generalized position (the fields themselves) and momentum variables (the conjugate field momenta), and then re-write *that* expression in terms of the Lagrangian. (We present here a brief description of the process. For a complete argument, please see [2].) To do this, we form the generalized version of (4), which is

$$U(q_a, q_b; T) = \langle q_b | e^{-iHT/\hbar} | q_a \rangle. \quad (7)$$

We then break the time interval T into N slices of arbitrarily small duration, ϵ . This eventually leads to a functional (path) integral expression for U that involves N coordinate integrals and N momentum integrals:

$$U(q_a, q_b; T) = \left(\prod_j \int \mathcal{D}q(t) \mathcal{D}p(t) \right) \exp \left[\frac{i}{\hbar} \int_0^T dt \left(\sum_j p^j \dot{q}^j - H(q, p) \right) \right]. \quad (8)$$

Here, the functional (path) integrals are standard integrals over the entire phase space. That is,

$$\prod_j \int \mathcal{D}q(t) \mathcal{D}p(t) = \prod_j \int \frac{dq^j dp^j}{2\pi\hbar}$$

at each point in time.

The extension to quantum field theory is achieved by observing that (8) should hold for any quantum system, including, for instance, a scalar field. To quantize a real scalar field $\phi(x)$, then, we note that in field theory our coordinates q^j are what are known as field amplitudes $\phi(\mathbf{x})$. Thus, (7) and (8) become

$$\langle \phi_b(\mathbf{x}) | e^{-iHT/\hbar} | \phi_a(\mathbf{x}) \rangle = \int \mathcal{D}\phi \exp \left[\frac{i}{\hbar} \int_0^T d^4x \mathcal{L} \right], \quad (9)$$

where we have explicitly referenced the four space time coordinates of our field, and where \mathcal{L} is the Lagrangian density, which in this case is

$$\mathcal{L} = \frac{1}{2} (\partial_\mu \phi)^2 - V(\phi). \quad (10)$$

We immediately see that (9) looks very similar to a partition function \mathcal{Z} in statistical mechanics, where the functions of our functional are our states, each of which is appropriately weighted by a Boltzmann weight $e^{iS[x^\mu]/\hbar}$. We can thus write

$$\mathcal{Z} = \int \mathcal{D}\phi \exp \left[\frac{i}{\hbar} \int_0^T d^4x \mathcal{L} \right] \quad (11)$$

Note that we have thus far been determining how to formulate quantum field theories. The remarkable aspect of using path integral formalism within such quantum field theories is that only *classical* fields have to be considered. To simulate a field theory defined as such on a computer, in order to also cover non-perturbative effects, we can exploit the continuity of the classical fields. Computers favor discretized, Euclidean systems. Our field, though, is currently formulated in Minkowski space. What we need, then, is to perform a Wick rotation of the time coordinate $t \rightarrow -ix^0$. This alleviates the need to resort to contour integration to evaluate the integral in (11), because we now have a *Euclidean* 4-vector norm:

$$x^2 = t^2 - |\mathbf{x}|^2 \rightarrow -(x^0)^2 - |\mathbf{x}|^2 = -|x_E|^2. \quad (12)$$

After performing the Wick rotation we obtain the partition function in Euclidean time,

$$\mathcal{Z} = \int \mathcal{D}\phi \exp \left[-\frac{1}{\hbar} \int d^4x_E \mathcal{L}_E \right] \equiv \int \mathcal{D}\phi e^{-S}. \quad (13)$$

We note that by adding source field terms \mathcal{Z} can be made into a “generating functional of correlation functions” ([2], p292). From this generating functional, the physically relevant correlation functions can be determined which correspond to the Green’s functions in Minkowski space. We now have a path integral formulation of a Euclidean partition function that can in principle be used to describe any field theoretical system.

Recall from statistical mechanics that the partition function is used to compute the expectation value of an arbitrary observable (or operator corresponding to any physically observable states of a quantum system) $\langle O[\phi] \rangle$ as follows:

$$\langle O[\phi] \rangle = \frac{\int \mathcal{D}\phi O[\phi] e^{-S[\phi]}}{\int \mathcal{D}\phi e^{-S[\phi]}}. \quad (14)$$

Instead of talking about a *path* as we did in the quantum mechanical case, we now use the notation of *configurations of fields*, over which we integrate in our path integral. In the discretized version, each possible configuration is, as mentioned, weighted by the appropriate Boltzmann factor and so, for our purposes, (14) becomes simply a summation of the values of our observable determined over all configurations generated according to the probability distribution e^{-S} of our lattice, divided by the total number of configurations:

$$\langle O[\phi] \rangle = \frac{\sum O[\phi] e^{-S[\phi]}}{\sum e^{-S[\phi]}} = \frac{1}{N_{conf}} \sum_{conf} O[\phi]. \quad (15)$$

(The actual calculation in (15) is accomplished via numerical simulations using the concept of *importance sampling*. In this report we cannot provide a comprehensive discussion of the simulation techniques and refer to [3] for more details.)

2.2 Topological Susceptibility

2.2.1 Topological charge

The *topological charge* Q of a lattice configuration is a concept that arises naturally in the treatment of gauge field theories. The topological charge characterizes purely topological properties of the gauge fields and can be interpreted as a winding number. The topological charge plays an important role in quantum chromodynamics (QCD), which is the field theoretic description of the strong force interactions between gluons and quarks inside hadrons. Investigating QCD upon a lattice involves discretizing otherwise continuous fields and then recovering the continuum limit by allowing the spacing between lattice points, a , to approach zero and the number of points upon the lattice, N , to approach infinity such that the physical extent L of our lattice remains constant, i.e., $L = Na = \text{const}$. A complete description of lattice QCD is beyond the scope of this paper, so we instead present here only a motivation for our project.

Although we are ultimately interested in a full treatment of QCD itself, this theory is rather complex and very demanding to simulate. Fortunately, there is a lower, namely 2-dimensional, model, the Schwinger model, which exhibits a number of properties it shares with QCD, most notably the confinement of quarks. What is of interest for us here is that also in the Schwinger model the concept of topological charge can be introduced and, hence, topological properties can be studied. In fact, since the Schwinger model is much simpler to simulate than QCD, it provides an ideal arena in which to address such questions.

The particular problem we want to investigate in this work is the behavior of the topological charge and the so-called topological susceptibility towards the continuum limit. We will compare two definitions of the topological charge. One of them originates from the purely fermionic sector of the theory while the other stems from the gauge field part only. The main motivation for studying the topological susceptibility is that it determines the mass of the η' meson which is hence – and quite intriguingly – of a purely topological nature. The continuum action for the Schwinger model can be written [4] [5] as

$$S_{Schw,ferm} = \int d^2x \left[\frac{1}{4} F_{\mu\nu} F_{\mu\nu} + \bar{\psi} (\gamma_\mu D_\mu + m) \psi, \right] \quad (16)$$

where $F_{\mu\nu}$ is the electromagnetic field strength tensor,

$$F_{\mu\nu} = \partial_\mu A_\nu - \partial_\nu A_\mu,$$

the ψ fields represent the fermions on the lattice, the γ_μ correspond to an appropriate representation of the Pauli spin matrices, and D_μ is the so-called Dirac operator which depends on the gauge fields A_μ as

$$D_\mu = \partial_\mu + ieA_\mu, \quad (17)$$

with e the physical charge of the fermions. We will not provide a detailed description of how to discretize this model on a lattice but just mention that instead of the charge e a dimensionless coupling $\beta \equiv 1/e^2 a^2$ is considered on the lattice. Note that $\beta \propto 1/a^2$ and hence, the continuum limit $a \rightarrow 0$ is reached by sending $\beta \rightarrow \infty$.

We must first provide the two definitions of the topological charge we have used. The *pure gauge field* definition of topological charge is given by

$$Q_{gauge}(A) \equiv \frac{e}{4\pi} \int d^2x \epsilon_{\mu\nu} F_{\mu\nu}(x), \quad (18)$$

where $\epsilon_{\mu\nu}$ is a two-index ϵ tensor. It can be shown that this integral gives only integer numbers (which, incidentally, represent the *winding number* of the gauge field).

The second definition of the Dirac operator describes the interaction of the fermion fields. In order to arrive at the fermionic definition of the topological charge, we have to define an *overlap operator* D_{ov} in terms of our original Dirac operator D :

$$D_{ov} \equiv 1 - \frac{D}{\sqrt{D^\dagger D}}. \quad (19)$$

(For the full derivation of D_{ov} we refer to reader to the literature, e.g., [6] [7].)

The important property of the overlap operator is the following: If we consider an eigenvalue problem

$$D_{ov}\phi_{ov} = \lambda_{ov}\phi_{ov} \quad (20)$$

and we are looking for only the zero mode solutions with the additional property that these zero modes are chiral, i.e. they obey

$$\sigma_3\phi_{ov} = \pm\phi_{ov}. \quad (21)$$

then the overlap operator indeed admits such solutions *even on the lattice*. This is completely different from other choices of lattice Dirac operators which do not have such solutions.

The zero modes of the overlap operator allow us to define the *index of the Dirac operator* and, hence, the index of our configuration: The index is the number of zero modes n_+ with positive chirality minus the number of zero modes n_- with negative chirality. The key point is that the index provides an *alternative definition* of the topological charge Q_{ferm} which is now obtained from the fermions only:

$$index(D) \equiv n_+ - n_- = Q_{ferm}. \quad (22)$$

The remarkable connection between the topological charge originating from the

pure gauge fields and pure fermions is given in the Atiyah-Singer Index Theorem, which states that these two definitions are equivalent [5]:

$$Q_{gauge} \equiv \frac{e}{4\pi} \int d^2x \epsilon_{\mu\nu} F_{\mu\nu}(x) = index(A) \equiv Q_{ferm}. \quad (23)$$

2.2.2 Topological susceptibility

Although the topological charge characterizes the topological properties of a gauge field configuration, it is the topological susceptibility which is of direct physical relevance.

The topological susceptibility χ_{topo} in the 2-dimensional abelian Schwinger model in Euclidean space is defined as

$$\chi_{topo} = \int \langle Q(x)Q(0) \rangle d^2x \quad (24)$$

where the $Q(x)$ is the topological charge density which is given from the pure gauge definition as:

$$Q(x) = \frac{e}{2\pi} F_{12}(x) = \frac{e}{2\pi} \left(\partial_1 A_2(x) - \partial_2 A_1(x) \right). \quad (25)$$

What can be seen from these formulae is that the topological susceptibility is a measure of the fluctuations of the topological charge. Hence, it can also be determined from the fermionic definition of the topological charge. To be more precise, the topological susceptibility using the Ginsparg-Wilson Dirac operator can be computed as follows:

$$\chi = \lim_{V \rightarrow \infty} \frac{\langle (n_R - n_L)^2 \rangle}{V} \quad (26)$$

where $\langle (n_R - n_L)^2 \rangle$ is the expectation value of the square of the index of the Ginsparg-Wilson fermion Dirac operator, and V is the physical volume of the lattice. This allows us to compare the topological susceptibility from both definitions of the topological charge.

The physical relevance of the topological charge susceptibility is encoded in the famous Witten-Veneziano formula [8] which relates it to the η' meson:

$$m_{\eta'}^2 = \frac{2N_f}{F_\pi^2} \chi_{topo} \quad (27)$$

This formula represents a second most remarkable example that fermionic quantities (here the η' mass) can be directly computed from pure gauge observables. The other example we presented in this report has been the Atiyah-Singer index theorem.

In terms of [9], the theory predicts that the value of the topological charge susceptibility in the continuum limit equals $\frac{1}{4\pi^2} = 0.02533$.

Our aim was to investigate the topological susceptibility χ_{topo} using the aforementioned two different definitions of Q and to both verify the predicted value in the continuum limit for the quenched model and determine the extent to which the two definitions agreed. The program we used to perform these simulations utilizes the Metropolis and Hybrid Monte Carlo algorithms. For details, please see the 2006 summer student report by Marinkovic and Nube [10].

3 Results

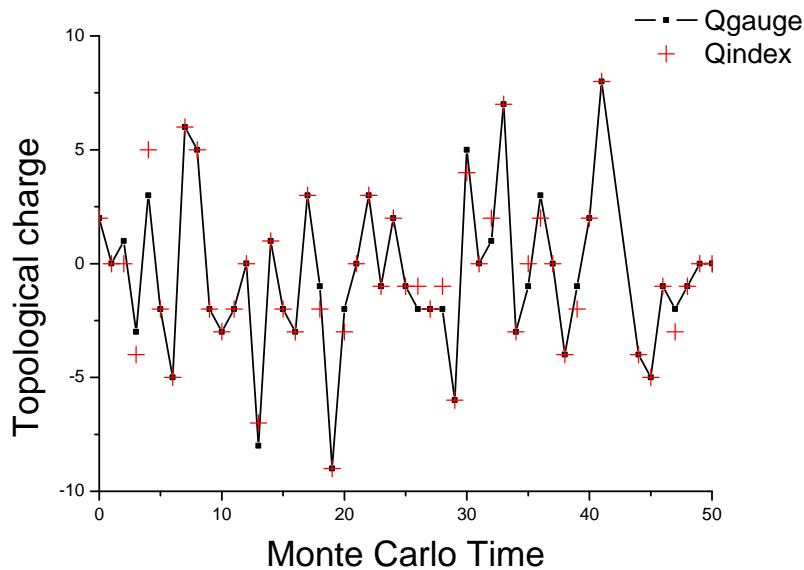


Figure 1. Dependence of topological charge on the Monte Carlo Time.

To test the extent to which the two definitions of topological charge differed, we simply plotted the value of Q as a function of Monte Carlo time for the two definitions upon the same lattice. An example is presented in Figure 1, for $\beta = 3.375$ (Recall that $\beta \equiv 1/a^2$). It can be seen that in most of the cases the topological charge agrees but that there are some occasions where we observe a difference. We will make this statement more quantitative below. To make our measurements more precise and to be sure that successive lattice configurations were independent from each other, we calculated an autocorrelation value for each lattice size and found that it was not always equal to one. To correct for this, we instructed our simulation to generate and then discard the appropriate number such that the measured autocorrelation time τ_Q has been $\tau_Q \approx 1$. We remark that for larger values of β the number of discarded configurations

increased. From the plot it is indicative that the values of topological charge are independent and they change rapidly. Note that there are a lot of fluctuations around the mean value of zero such that we can be sure to really sample sufficiently many sectors of the topological charge.

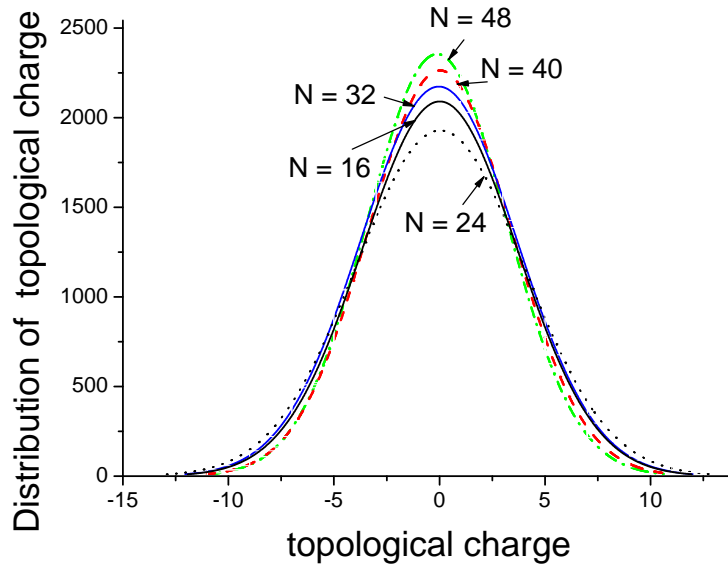


Figure 2. Distribution of topological charge.

On Figure 2 is presented the distribution of the topological charge of a fixed physical volume lattice for different numbers of lattice points $N = 16, 24, 32, 40, 48$. A fixed physical volume means that $V = L^2 = (Na)^2 = \frac{N^2}{\beta} = \text{constant}$. The constant has been determined such that we have chosen $N = 48$ for $\beta = 6$. Corresponding β values for the different values of N given above were calculated for this fixed lattice volume constraint. As expected, the distribution is uniform and with a mean value equal to zero.

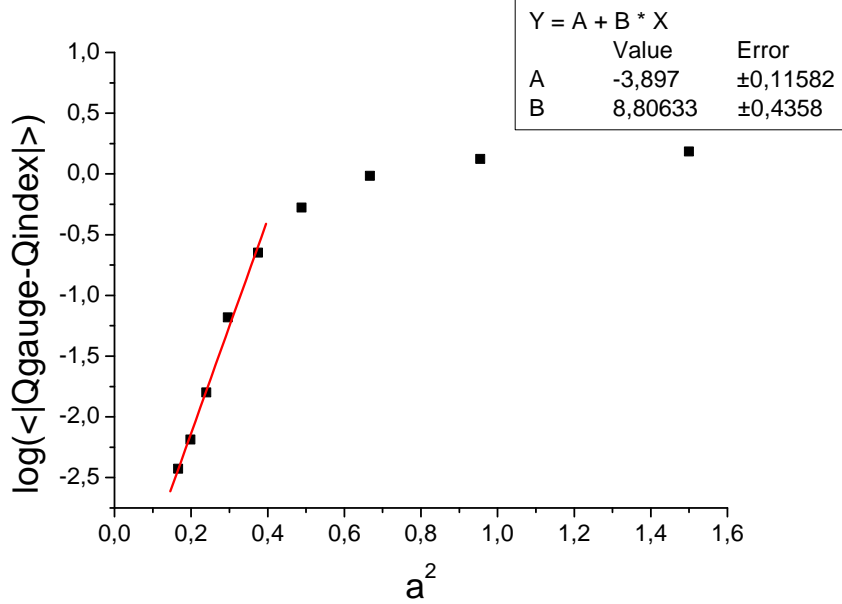


Figure 3. Change in $\langle |Q_{gauge} - Q_{index}| \rangle$ vs. $\frac{1}{\beta}$.

From the arguments above one can expect that the two values of the topological charge from our two definitions should coincide in the continuum limit. At a non-vanishing lattice spacing, the values for the topological charge can differ. The most interesting thing here is therefore to investigate how the difference between the topological charges changes as we vary the number of lattice points and hence, since we work in a fixed physical volume, the lattice spacing. Figure 3 is a plot of $\log(\langle |Q_{gauge} - Q_{index}| \rangle)$ versus $\frac{1}{\beta} \propto a^2$. Here one can observe a linear behavior of the expectation value of the topological charge difference from the two definitions versus a^2 . In the continuum limit when $a^2 \propto \frac{1}{\beta} \rightarrow 0$, these two definitions should give the same value according to the Atiyah-Singer Index Theorem. That means that in the continuum limit as $a^2 \rightarrow 0$ the mean of the absolute value of the difference between these two topological charges should go to zero. As one can see on this plot, the logarithm of the difference decreases linearly indicating that the difference of the topological charge from both definitions vanishes exponentially fast. The linear regression yields the following : $y = -3.9 + 8.8 a^2$. This indicates that the difference approaches zero in a very rapid way; it behaves like

$$(const) e^{-8.8a^2}.$$

It is unclear why there should be this exponential behavior, but we present a possible argument here. As will be shown below, from the comparison of the

topological charge susceptibility from two definitions, one can consider χ_{topo} versus the value $a^2 < 0.4$ in the following way:

$$\chi_{gauge} = \chi^{cont} + (const) a^2 + \dots \quad (28)$$

$$\chi_{index} = \chi^{cont} + (const)' a^2 + \dots \quad (29)$$

For $a^2 < 0.4$ we see that $(const) \approx (const)'$ and if one calculates the difference of the topological charge $\langle |Q_{gauge} - Q_{index}| \rangle$, it becomes apparent that a^2 dependence for the difference is canceled out. It is possible, of course, that many of the higher-order corrections in a might cancel, too. This suggests an explanation for the exponentially fast decrease of the difference of topological charge which is an even better result than we expected.

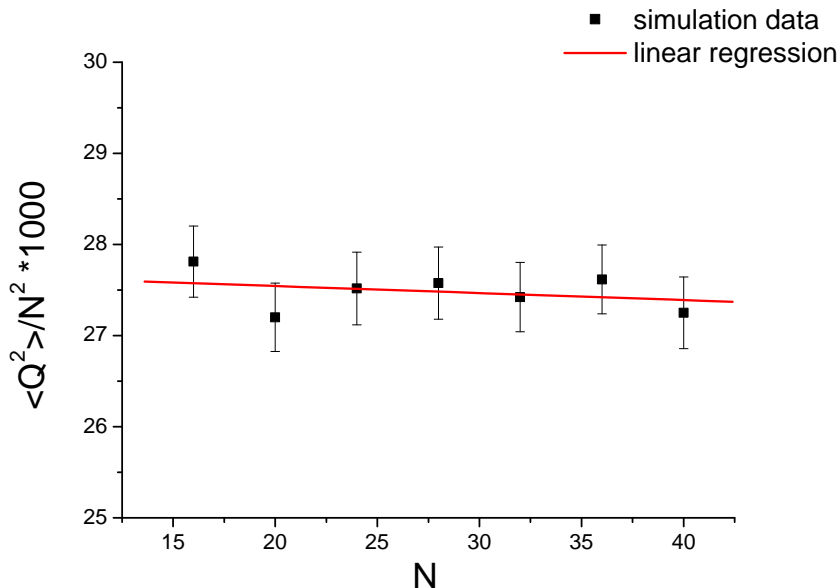


Figure 4. Dependence of topological charge susceptibility on the number of lattice points.

Figure 4 shows the dependence of topological charge susceptibility versus the lattice size. This is a check to see if the lattices we use in our simulations are large enough to be considered comparable to the one with infinite volume. This investigation will ensure us that lattice size doesn't influence the value of topological charge susceptibility. To perform the check, we fixed one of the β values (here $\beta = 1.5$) and varied the number of lattice points over $N = 16, 20, 24, 32, 36, 40$. From the plot it is clear that the value of topological charge

susceptibility χ_{topo} changes very lightly and within the limits of error it is a constant value. This means that the volume was chosen large enough.

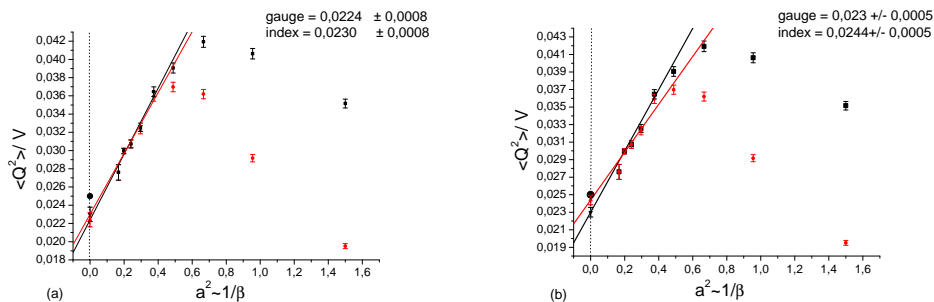


Figure 5. Dependence of topological charge susceptibility on $1/\beta$, from two definitions. The black point at zero represents the theoretically expected value of $1/4\pi^2$.

On Figure 5 one can observe how the topological charge susceptibility changes as $1/\beta$. Here we perform a linear fit in a^2 to our data of topological charge susceptibility χ_{topo} for both of our definitions, that of the pure gauge theory and that of the fermionic definition using the overlap operator. Graph (a) shows the fit for 5 lattice sizes ($N = 32, 36, 40, 44,$ and 48) and (b) for the linear fit with the inclusion of 6 lattice sizes (the same as before, adding $N = 28$). These plots suggest that in the continuum limit and within one or two standard deviations, both definitions provide the same value of topological charge susceptibility. Although this has been expected, it is a highly non-trivial check. The theoretical prediction of $1/4\pi^2$ [9] was also made with some assumptions and is thus expected to be only approximately true, itself. Therefore, our simulations provide a check on this theoretical prediction and check the underlying assumptions that led to the theoretical value.

Below the table of topological charge susceptibility values is presented, along with χ^2 goodness-of-fit values.

Number of points	Gauge $\langle Q^2_{(continuum)} \rangle / V$	Index $\langle Q^2_{(continuum)} \rangle / V$	χ^2_{gauge}	χ^2_{index}
5	0.0224 ± 0.0008	0.0230 ± 0.0008	5.6	5.3
6	0.0230 ± 0.0005	0.0244 ± 0.0005	6.7	11.6

It can be seen that all the values agree within the errors. Further, whether or not we find a deviation from the theoretically expected value is hard to judge given our present error bars. It is, however, interesting to note that we see indications that the theoretical value overshoots the simulation data.

We finish this section with two comments. The first is that, very remarkably, the continuum limit of the topological susceptibility is reached in a non-monotonous way. Second, even if we are in a regime of the data where the data scale with an a^2 behavior to zero, the effects of the lattice spacing can be very large and the value of the topological susceptibility on the lattice can be almost twice as large as the continuum value. This is a surprisingly large effect for the Schwinger model.

4 Conclusions and Future Work

During our work we made calculations on a fixed volume lattice at various β values. We computed the topological charge and the topological susceptibility by performing measurements on lattice, properly taking autocorrelation times into account. To compute the topological charge we used two definitions, one pure gauge one and a fermionic one defined through the index of the overlap operator. It was shown that the expectation value of the topological charge difference from two definitions versus lattice spacing a^2 has a very steep dependence and approaches zero exponentially fast and hence more rapidly than expected. We also demonstrated that our chosen fixed volume size has been chosen large enough to not influence our results. We found that in the continuum limit, within the errors, the two definitions of the topological charge susceptibility coincide. The result of our simulations could not finally clarify whether the theoretical prediction is indeed correct or not.

However, as all our investigations show, we need much better statistics, especially for large values of β . These simulations are, in fact, currently running. These measurements will allow us to more confidently assert the agreement or disagreement with the value predicted in [9], and will pave the way for a rigorous calculation of the mass of the η' meson predicted by the Witten-Veneziano formula [8].

Acknowledgments

We wish to heartily thank Karl Jansen for his stewardship and patience on all levels and at all times, Andreas Nube for his willingness to explain and re-explain programming concepts and issues (and to whip up necessary scripts at a moment's notice), and everyone at DESY Zeuthen for their support and good humor.

References

- [1] R. P. Feynman and A. R. Hibbs, *Quantum Mechanics and Path Integrals* (McGraw-Hill, New York, 1965).
- [2] M. E. Peskin and D. V. Schroeder, *An Introduction to Quantum Field Theory* (Westview Press, Boulder, CO, 1995).
- [3] M. Creutz and B. Freedman, *Annals of Physics* **132**, 427 (1981).
- [4] J. Schwinger, *Phys. Rev.* **128**, 2425 (1962).
- [5] L. Giusti, C. Hoelbling, and C. Rebbi, *Phys. Rev. D* **64**, 054501 (2001).
- [6] N. Christian, K. Jansen, K. Nagai, and B. Pollakowski, *Nuclear Physics B* **739**, 60 (2006).

- [7] P. Hernandez, K. Jansen, and L. Lellouch, *Physics Letters B* **469**, 198 (1999).
- [8] S. Azakov, H. Joos, and A. Wipf, *Physics Letters B* **479**, 245 (2000).
- [9] L. Giusti, G. C. Rossi, M. Testa, and G. Veneziano, *Nuclear Physics B* **628**, 234 (2002).
- [10] M. Marinković and A. Nube, “Localization and Evolution of Quark Fields”, DESY Zeuthen Summer Student Program Report, 2006.